The Capitanian Minimum: A Unique Sr Isotope Beacon of the Latest Paleozoic Seawater

Tomomi Kani[1]* and Yukio Isozaki[2]

[1]Division of Natural Science Earth and Environmental Science, Faculty of Advanced Science and Technology, Kumamoto University, Kumamoto, Japan, [2]Department of Earth Science and Astronomy, The University of Tokyo, Komaba, Tokyo, Japan

The long-term trend in the Paleozoic seawater $^{87}Sr/^{86}Sr$ was punctuated by a unique episode called the "Capitanian minimum" at the end of the Guadalupian (Permian; ca. 260 Ma). This article reviews the nature and timing of this major turning point in seawater Sr isotope composition ($^{87}Sr/^{86}Sr$, $\delta^{88}Sr$) immediately before the Paleozoic-Mesozoic boundary (ca. 252 Ma). The lowest value of seawater $^{87}Sr/^{86}Sr$ (0.7068) in the Capitanian and the subsequent rapid increase at an unusually high rate likely originated from a significant change in continental flux with highly radiogenic Sr. The assembly of the supercontinent Pangea and its subsequent mantle plume-induced breakup were responsible for the overall secular change throughout the Phanerozoic; nonetheless, short-term fluctuations were superimposed by global climate changes. Regarding the unidirectional decrease in Sr isotope values during the early-middle Permian and the Capitanian minimum, the suppression of continental flux was driven by the assembly of Pangea and by climate change with glaciation. In contrast, the extremely rapid increase in Sr isotope values during the Lopingian-early Triassic was induced by global warming. The unique trend change in seawater Sr isotope signatures across the Guadalupian-Lopingian Boundary (GLB) needs to be explained in relation to the unusual climate change associated with a major extinction around the GLB.

Keywords: Sr isotope, seawater, Capitanian, Permian, continental crust, Pangea, climate change, carbonate

INTRODUCTION

The fluctuations in seawater $^{87}Sr/^{86}Sr$ values throughout Earth's history are archived in ancient carbonates and have been strongly linked to global phenomena, such as changes in global tectonics and climate change (e.g., Veizer and Compston 1974; Burke et al., 1982; DePaolo and Ingram, 1985; Richter and Depaolo, 1988; Hess et al., 1986; Hess et al., 1989; Veizer, 1989; Richter et al., 1992; Holland, 2003; McArthur et al., 2012). The $^{87}Sr/^{86}Sr$ ratio of modern seawater is globally uniform, and the major fluxes driving the seawater ratio are threefold; 1) weathering of highly radiogenic silicates and less radiogenic carbonates on continents, 2) nonradiogenic submarine hydrothermal fluid from mid-oceanic ridges (MORs), and 3) weathering of less radiogenic basalts of island arcs and oceanic islands (e.g., Allègre et al., 2010). Continuous stratigraphic sequences of unaltered carbonates provide the best records of the Sr isotope compositions of ancient seawater and their secular changes, which have been controlled solely by nonbiological processes. This is a great advantage of Sr isotope data in paleoenvironmental research with respect to other isotopic proxies, such as $\delta^{13}C$, $\delta^{15}N$, and $\delta^{34}S$, which reflect mass-dependent isotope fractionation through various biological processes.

FIGURE 1 | Overview of Phanerozoic seawater ^{87}Sr/^{86}Sr and δ^{88}Sr profiles with major extinction timings, secular changes in sea level, glacial episodes and the assembly and breakup of the supercontinent Pangea. ^{87}Sr/^{86}Sr and δ^{88}Sr profiles are modified from McArthur et al. (2012) and Vollstaedt et al. (2014). The secular change in sea level is modified from Haq and Schutter (2008). Vertical light gray and blue bars represent are cold and glacial episodes, respectively (Dera et al., 2011; Friedrich et al., 2012; Montanez and Poulsen, 2013; Bodin et al., 2015; Montanez, 2016; Fielding et al., 2008; Metcalfe et al., 2015).

Overall, the seawater Sr isotope ratio during the Phanerozoic is characterized by two trends, i.e., the long-term decrease in the entire Paleozoic and the long-term increase in the Mesozoic-Cenozoic, with small scale fluctuations of ca. 100 m.y. cycles (e.g., McArthur et al., 2012; **Figure 1**). The most unique aspect of Phanerozoic Sr isotope values is the major trend change that occurred in the latest Paleozoic to early Mesozoic, which is marked by two episodes of the lowest Sr isotopic value: one in the Capitanian (late Guadalupian, Permian) and the other at the Middle-Late Jurassic transition. During these episodes, seawater ^{87}Sr/^{86}Sr values decreased to 0.7068, hitting their minimum in the Phanerozoic. These values clearly recorded the suppression of continental flux with highly radiogenic Sr with respect to the nonradiogenic hydrothermal flux from MORs. The Jurassic episode has been reasonably explained as a direct result of the opening of the Atlantic Ocean in the framework of the major breakup of the supercontinent Pangea with the generation of new continental margins. In contrast, the Permian case remains

debatable because no apparent coincidence with major continental breakup is confirmed. This episode surely recorded a relatively small continental flux into the global seawater with respect to the hydrothermal flux from ocean floors; nonetheless, the driving factor of this decrease has not yet been identified.

Notably, a major climate change and biodiversity crisis occurred near the end of the Guadalupian (ca. 260 Ma; e.g., Jin et al., 1994; Stanley and Yang, 1994; Isozaki and Ota, 2001; Bambach, 2002; Wang et al., 2004; Bond et al., 2010; Wignall et al., 2012; Rampino and Shen 2019; Lucas, 2021), ca. 8 m.y. before the well-known major extinction across the Permo-Triassic (Paleozoic-Mesozoic) boundary (ca. 252 Ma); however, the main cause of the end-Guadalupian extinction remains unidentified, although coeval geological phenomena are emphasized, including the significant change in seawater Sr isotopes and the lowest sea-level (e.g., Haq and Schutter, 2008; Isozaki, 2009; Kani et al., 2013; Kofukuda et al., 2014).

This review article documents the latest compilation of ^{87}Sr/^{86}Sr records of the Permian, particularly with the reappraisal of Sr
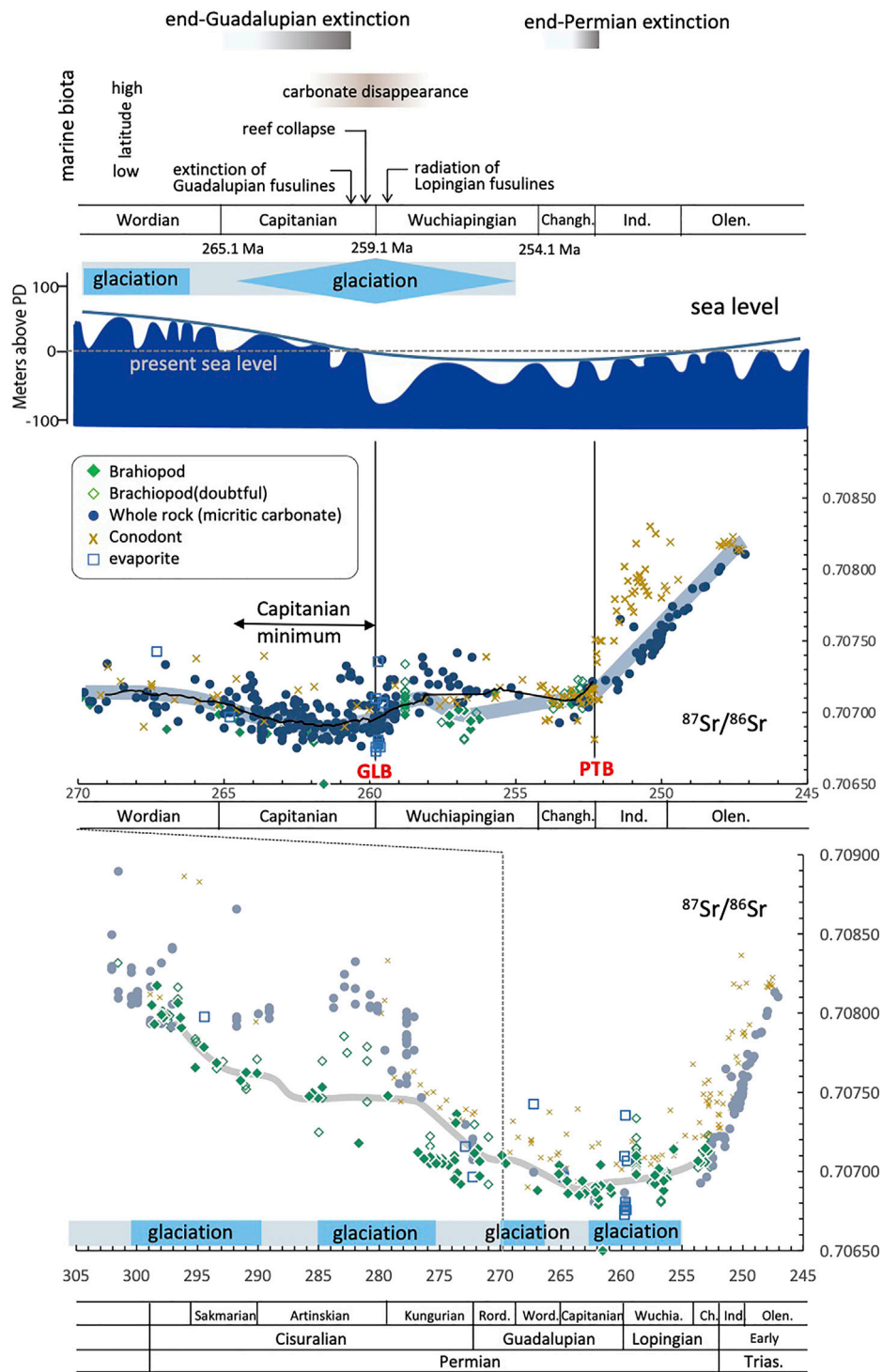
FIGURE 2 | A schematic correlation diagram showing an updated secular change in seawater Sr isotope values across the GLB, together with coeval global environmental changes, sea-level changes, and extinctions. $^{87}Sr/^{86}Sr$ curve (Upper): Values adopted from Veizer and Compston (1974), Denison et al. (1994), Martin and Macdougall (1995), Morante (1996), Korte et al. (2003), Korte et al. (2004), Korte et al. (2006), Kani et al. (2013), Sedlacek et al. (2014), Vollstaedt et al. (2014), Song et al. (2015), Wang et al. (2018), Kani et al. (2018), Li et al. (2020), Li et al. (2021). All data were adjusted to NIST SRM 987 = 0.710248 (McArthur et al., 2001) and recalculated according to the Geologic Time Scale 2012 (Gradstein et al., 2012). The black line is the running average of biostratigraphically well-defined (conodont biozonation) and well-preserved (diagenetically screened) brachiopod and conodont and well-defined (conodont or fusuline biozonation) whole rock (micritic carbonate) data with 2 m.y. time steps and a 3 m.y. window. $^{87}Sr/^{86}Sr$ curve (Lower): modified from Figure 2 in Korte and Ullmann (2016).

isotopic data from Permian carbonates deposited in various settings in the world, especially with new data from South China, Japan, and Primorye (Far East Russia). $^{87}Sr/^{86}Sr$ isotope data from skeletal and bulk micritic carbonate samples are also comparatively evaluated. In addition, coeval Permian tectonic/climatic regimes are discussed in relation to their possible influences on secular changes in $^{87}Sr/^{86}Sr$ and $\delta^{88}Sr$ isotopic systems.

V-SHAPED TREND CHANGE IN CAPITANIAN SEAWATER $^{87}SR/^{86}SR$

Overall Aspect

The overall Permian profile of the seawater Sr isotope ratio is characterized by a sharp V-shaped pattern formed by a long-term decrease during the Cisuralian-Guadalupian and a rapid increase in the Lopingian-Early Triassic. The lowest value of $^{87}Sr/^{86}Sr$ occurred in the Capitanian (late Guadalupian; 265–260 Ma) (**Figure 1**), which recorded the major change in weathering related to climate change or global tectonics (e.g., Veizer, 1989; Veizer et al., 1999; Korte et al., 2003; Banner, 2004; Korte et al., 2003; Kani et al., 2008; McArthur et al., 2012; Kani et al., 2013).

The entire Permian best-fit curve was demonstrated by Korte and Ullman (2016), on the basis of the data from well-preserved brachiopod shells and biostratigraphically well-defined conodonts data from Korte et al. (2006), which are regarded to represent the most reliable Sr isotope recorder of ancient seawater. The $^{87}Sr/^{86}Sr$ values of conodonts during the late Permian were updated by those of biostratigraphically re-defined conodonts reported by Song et al. (2015). Almost all the data from Capitanian brachiopods show extremely low $^{87}Sr/^{86}Sr$ values less than 0.7070 down to 0.7068. In contrast, the $^{87}Sr/^{86}Sr$ values of Wuchiapingian brachiopods show a rapid increase up to 0.7072. The coeval $^{87}Sr/^{86}Sr$ values measured for whole-rock samples of fine-grained limestone (micrite) generally agree with those of brachiopods. **Figure 2** (upper) displays the $^{87}Sr/^{86}Sr$ curve compiled from previous data (**Supplementary Table S1**; references in Korte and Ullman 2016; Kani et al., 2008; Kani et al., 2013; Song et al., 2015; Kani et al., 2018; Wang et al., 2018; Li et al., 2020; Shen et al., 2020) from samples of biostratigraphically dated and well-preserved (diagenetically screened) brachiopod shells, conodonts and micrite samples. When Burke et al. (1982) first reported the Phanerozoic Sr isotope curve as a global seawater signal, nonmetamorphosed micrite samples were regarded to be promising for high-resolution Sr isotope stratigraphic correlation because a good correlation was confirmed between the brachiopod shell and associated micrites. As whole-rock analysis of micrite samples potentially has uncertainty, careful treatments are needed before dissolving in dilute suprapure acetic acid, e.g. hand-picking of millimeter-sized grains of micrite under a microscope for screening dolomitized and/or other diagenetic products; nonetheless, this approach is still practical for nonfossiliferous limestone intervals and/or horizons.

Decrease in the Cisuralian-Guadalupian

According to the compilation of Permian $^{87}Sr/^{86}Sr$ secular evolution by Korte and Ullmann (2016), the Late

Carboniferous–middle Permian trend is represented by an unidirectional decrease in $^{87}Sr/^{86}Sr$ that stops in the Capitanian (late middle Permian) (Burke et al., 1982; Denison et al., 1994; Morante 1996; Korte et al., 2006; Kani et al., 2008; Wignall et al., 2009; Shen and Mei, 2010; Tierney 2010; Kani et al., 2013; Liu et al., 2013). The Asselian-Capitanian $^{87}Sr/^{86}Sr$ decrease is characterized by a rapid rate of approximately 0.0003/ 10 m.y.(from 0.7080 to 0.7069 in 35 m.y.), and the curve displays a stepwise-shape; the Asselian–Sakmarian and Wordian–Capitanian are the two steep stages (Korte et al., 2006; McArthur et al., 2012). The Capitanian minimum (~0.7069) marks the termination of the decrease, and the extremely low value lasted the entire Capitanian (ca. 5 m.y.) (Kani et al., 2008; Kani et al., 2013). The average of reliable brachiopods was 0.70684 ± 0.00015 [standard deviation (SD), n = 6] (data from Korte et al., 2006) and the average of all types of carbonates was 0.70694 ± 0.00012 (SD, n = 147; data from Denison et al., 1994; Martin and Macdougall, 1995; Morante, 1996; Korte et al., 2006; Wang et al., 2018; Kani et al., 2008; Kani et al., 2013; Kani et al., 2018) in the Capitanian, equal to the minimum values in the Mesozoic curve (0.70683, the early-middle Oxfordian transition, Late Jurassic) (Wierzbowski et al., 2017) as the lowest $^{87}Sr/^{86}Sr$ ratios in the Phanerozoic.

Increase in the Late Lopingian to Early Triassic

The seawater $^{87}Sr/^{86}Sr$ rapidly increased across the GLB (**Figure 2**). In the early Wuchiapingian, the $^{87}Sr/^{86}Sr$ value started to increase after the remarkable trend change from the long-term decrease *via* the transitional phase during the Capitanian. The values decrease again in the mid-Wuchiapingian. The sharp increase of 0.0017 during ca. 5 m.y. from the end of the Changhsingian to the late Early Triassic. This sharp increase is noteworthy because its slope is much steeper than that in the Late Jurassic, which is 0.0003 during ca. 12 m.y. from the late Oxfordian to early Volgian, marking the most rapid increase in the Phanerozoic.

Capitanian Minimum

The overall trend in seawater $^{87}Sr/^{86}Sr$ ratios during the Paleozoic recorded the long-term unidirectional decline superimposed with short-term fluctuations. In contrast, the Mesozoic-Cenozoic trend is almost the opposite, i.e., unidirectionally increasing. In the Paleozoic, the short-term fluctuation in Sr record repeated 4 times with 4 minima, and the magnitudes of all shifts were more or less the same, except for the Capitanian minimum which is much larger than others (**Figure 1**). We infer that this anomalous signal may have been caused not by common reciprocal process worked throughout the Paleozoic but was amplified by another unique agent. A negative shift in $\delta^{13}C$ immediately before the GLB indicates that a major perturbation has occurred in the global carbon cycle (e.g., Wang et al., 2004; Kaiho et al., 2005; Isozaki et al., 2007; Saitoh et al., 2013). Several possible mechanisms for causing this perturbation were proposed; e.g., sea-level change (Wang et al., 2004), ocean stratification and anoxia (Isozaki et al., 2007; Tierney, 2010), methane release
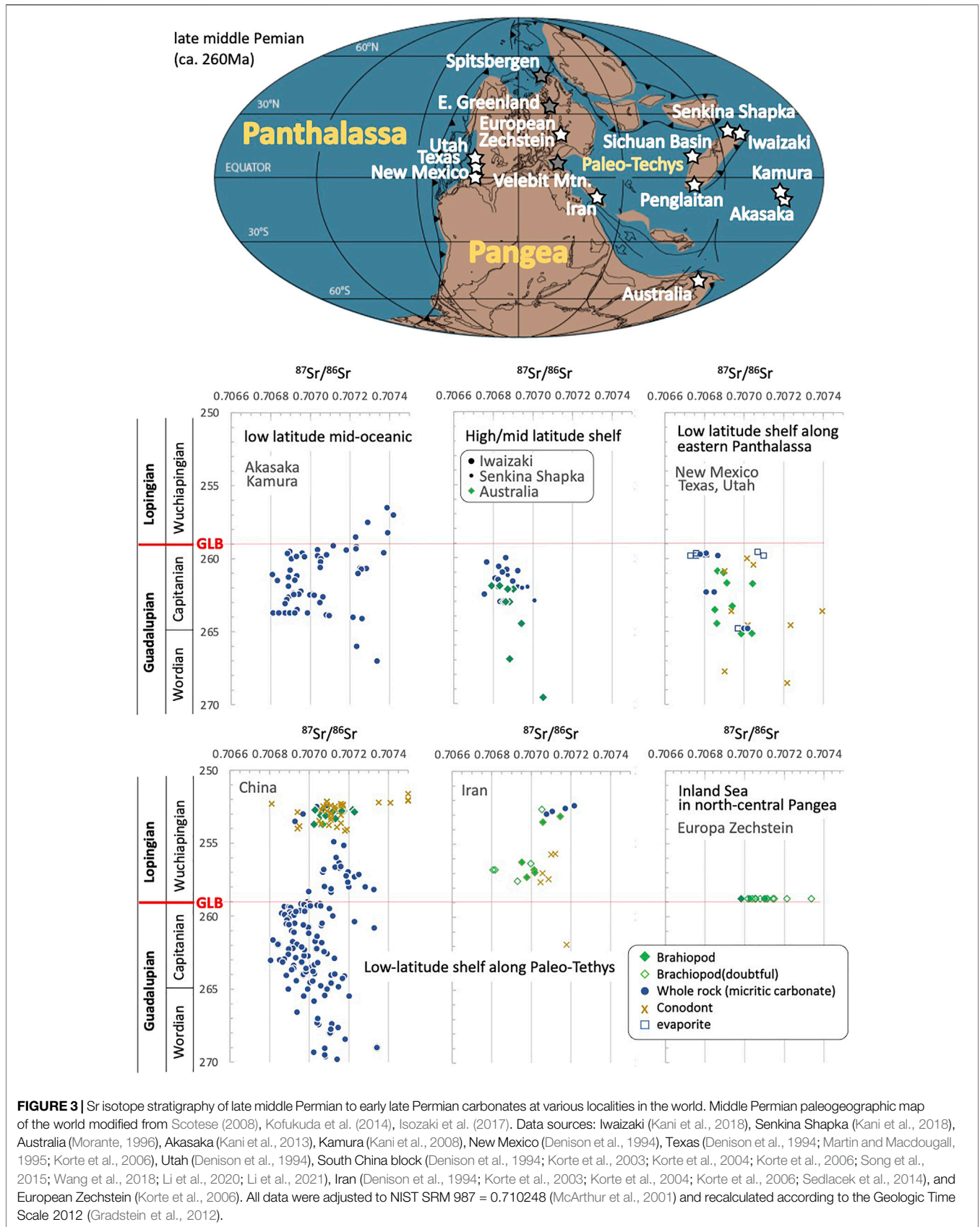
FIGURE 3 | Sr isotope stratigraphy of late middle Permian to early late Permian carbonates at various localities in the world. Middle Permian paleogeographic map of the world modified from Scotese (2008), Kofukuda et al. (2014), Isozaki et al. (2017). Data sources: Iwaizaki (Kani et al., 2018), Senkina Shapka (Kani et al., 2018), Australia (Morante, 1996), Akasaka (Kani et al., 2013), Kamura (Kani et al., 2008), New Mexico (Denison et al., 1994), Texas (Denison et al., 1994; Martin and Macdougall, 1995; Korte et al., 2006), Utah (Denison et al., 1994), South China block (Denison et al., 1994; Korte et al., 2003; Korte et al., 2004; Korte et al., 2006; Song et al., 2015; Wang et al., 2018; Li et al., 2020; Li et al., 2021), Iran (Denison et al., 1994; Korte et al., 2003; Korte et al., 2004; Korte et al., 2006; Sedlacek et al., 2014), and European Zechstein (Korte et al., 2006). All data were adjusted to NIST SRM 987 = 0.710248 (McArthur et al., 2001) and recalculated according to the Geologic Time Scale 2012 (Gradstein et al., 2012).

(Retallack et al., 2006; Retallack and Jahren, 2008; Bond et al., 2010), or Emeishan volcanism (Wei et al., 2012). Nonetheless, judging from less co-variation of carbon and calcium stable isotopes of carbonates and conodonts in China (Penglaitan and Chaotian), and Turky (Köserelik Tepe), Jost et al. (2014) concluded that the perturbation in the global carbon and calcium cycles across the GLB were less intense than those across the PTB, emphasizing the GLB event was less significant than PTB event. Nonetheless, Sr isotope records indicate the opposite, as marked by the most remarkable isotopic signature in the Paleozoic, i.e., the Capitanian minimum. Further analyses with multiple geochemical proxies in high resolution across the GLB are definitely needed to constrain extinction-relevant changes in seawater composition on a global scale.

PALEOGEOGRAPHY OF SR ISOTOPE RECORDS

Since pioneering studies in the SW United States (Denison et al., 1994; Martin and Macdougall, 1995), many attempts at seawater $^{87}Sr/^{86}Sr$ analyses for the Permian have been conducted mostly on carbonate sections, of which the distribution covers various regions in the world; i.e., North America, the Mid-East, Europe, Australia, and Asia (South China, Japan, and Far East Russia). From the perspective of paleogeography, the previously studied sections are widespread across the supercontinent Pangea as well as throughout the superocean Panthalassa (**Figure 3**). Their depositional settings are highly variable; i.e., continental shelf, intracontinental shallow sea, and mid-oceanic atoll. In addition, more differences exist among shelf sections in terms of paleolatitude (from low to high), ocean (Panthalassa, Tethys, or others), and longitudinal distribution of continental margins.

Regarding stratigraphic correlation and biostratigraphical dating, conodont fossils perform best with an average age resolution of approximately 1.3 m.y. (Korte et al., 2006; Henderson et al., 2012), although unavoidable problems relevant to faunal provincialism remain (Henderson and Mei, 2007). Among all sections, the Guadalupian sections in western Texas/New Mexico (United States) and the Penglaitan/Shanxi sections in South China with numerous fossil data and geochemical analyses are regarded as the most reliable reference sections for correlation (Shen et al., 2020). We also emphasize the significance of the unique records from mid-Panthalassa because they archive globally-averaged isotopic signatures of seawater without any influence from local tectonic disturbances in continental (Pangean) margins/interiors. This section briefly reviews the distribution of representative Capitanian sections with Sr isotope analyses, particularly those with newly added data.

Low-Latitude Shelf Along Eastern Panthalassa

The Permian marine sequences are exposed in the Permian Basin in west Texas and southern New Mexico, United States (Glenister et al., 1992), which include the Global Boundary Stratotype Section and Points (GSSPs) for the Rodian, Wordian and Capitanian Stages. These sequences represent low-latitude carbonate facies deposited along an embayment (Delaware Basin) on the western coast of Pangea (**Figure 3**). Sr records were reported by Denison et al. (1994), Martin and Macdougall (1995), and Korte et al. (2006).

Low-Latitude Shelf Along Paleo-Tethys

Thick fossiliferous shallow marine Permian carbonates are widely distributed in the northwestern part of South China. The South China (or Greater South China) was located in the low-latitude domain during the Permian between the Paleo-Tethys to the west and the Panthalassa to the east (**Figure 3**). The Guadalupian-Lopingian shallow marine carbonates, including the GSSP of the GLB at Penglaitan, have been analyzed by many researchers (e.g., Jin et al., 1994; Jin et al., 2006a). The Shansi section in Sichuan Province represents carbonates deposited on the Paleo-Tethys side, whereas those in Guanxi Province represents carbonates deposited on the Panthalassa side. In addition to classic datasets (Denison et al., 1994; Korte et al., 2003; Korte et al., 2004; Korte et al., 2006), detailed Sr isotope data were recently added by Song et al., 2015, Wang et al. (2018), Li et al. (2020), Li et al. (2021).

In addition, Capitanian carbonate-bearing sequences occur at Abadeh and Jolfa in Central Iran, Mid-East. These sections were deposited somewhere in the middle of the low-latitude Paleo-Tethys (**Figure 3**). The Guadalupian Abadeh Formation, and the overlying Lopingian Hambast Formation were analyzed for Sr isotopes by Denison et al. (1994), Korte et al. (2003), Korte et al. (2004), Korte et al. (2006), and Sedlacek et al. (2014).

Inland Sea in North-Central Pangea

The middle to late Permian sequence of inland-sea facies with evaporites is exposed in northern Germany and Poland. The depositional site (Zechstein Basin) was located in a low-latitude inland domain within the northern part of Pangea with a seaway connection to the Boreal Sea to the north (**Figure 3**). This basin was unique in depositing evaporites, such as bedded halite and anhydrites; however, carbonates are limited. Sr analyses were reported by Korte et al. (2006).

High-to Mid-Latitude Shelf Along the Western Panthalassa Margin

Capitanian shallow marine carbonate sequences of continental shelf facies are exposed in NE Japan and Far East Russia; e.g., at the Iwaizaki and Senkina Shapka, Primorye. Despite their current positions at mid-latitudes, these sections were primarily deposited at relatively low latitudes along Greater South China (**Figure 3**), as evidenced by fossils of warm water-adapted Tethyan biota (Zakharov et al., 1992; Kawamura and Machiyama, 1995; Shen and Kawamura, 2001; Kossovaya and Kropatcheva, 2013; Tobita et al., 2018). Sr isotope records from both sections were reported by Kani et al. (2018).

Low-Latitude Mid-Panthalassan Atoll

Numerous large and small Permian limestone blocks currently occur as exotic blocks within the Jurassic accretionary complexes

in Japan (Isozaki et al., 1990). They were primarily deposited on seamount tops as atoll complexes in the low-latitude mid-ocean of Panthalassa (**Figure 3**), as evidenced by abundant fossils of warm water-adapted biota, and secondarily transported by plate motion until their arrival at the active continental margin of Jurassic Japan (Pacific margin of Greater South China) (Isozaki, 1997; Sano and Nakashima, 1997). Some limestone blocks preserve continuous stratigraphic sections of Capitanian limestone and G-LB intervals, such as the Kamura and Akasaka limestones in SW Japan (Ota and Isozaki, 2006; Kasuya et al., 2012; Kofukuda et al., 2014). Sr isotope records from these two sections were reported by Kani et al. (2008) and Kani et al. (2013).

On the basis of these data from various parts of Pangea and Panthalassa/Paleo-Terthys, all reported Sr isotope data from the Capitanian and neighboring intervals are compiled in **Figure 3**. The overall trend of Permian seawater Sr isotope composition was confirmed and integrated by the present compilation with the latest data from South China, Japan, and Far East Russia. In short, we can conclude that the Permian seawater indeed shared the same Sr isotope composition worldwide, including the unique period around the GLB, regardless of paleogeographic positions, i.e., low-*vs.* high-latitude, Panthalassa *vs.* Paleo-Tethys, west (dry) side *vs.* east (wet) side of Pangea, mid-ocean *vs.* continental margin, etc.

SR BUDGET OF PERMIAN SEAWATER

According to Allègre et al. (2010), highly radiogenic Sr (^{87}Sr/^{86}Sr ratio of 0.7136) from continental weathering of carbonate (0.708) and silicate (0.721) contributes 34 and 25% of the Sr to modern seawater, respectively, whereas mantle-like nonradiogenic Sr (0.703) from submarine hydrothermal input and weathering of island arc or oceanic island basalts (0.7035) contributes 11 and 30%, respectively. The ^{87}Sr/^{86}Sr ratio in a river could have been controlled by the age of the rocks in its drainage basin (Goldstein and Jacobsen, 1987). The current flux of continental Sr to the ocean is quantified as a mixture of younger bedrock and older exorheic (ocean-connected) land area (Peucker-Ehrenbrinkand Fiske, 2019). However, the controlling factor of considerable changes in seawater ^{87}Sr/^{86}Sr compositions was weathering, especially age-integrated radiogenic silicate throughout the Permian because submarine hydrothermal activity could have remained at a constant low during the stable supercontinent period (Henderson et al., 2012).

It has been emphasized that the Capitanian minimum is particularly noteworthy because this episode recorded an extreme case in the seawater Sr budget during the last 500 m.y. with a possible connection to one of the large-scale mass extinctions. Nevertheless, the ultimate cause of this extreme condition at the end of the Paleozoic has not been identified, although some possible scenarios have been proposed, e.g., global tectonics with respect to continent configuration, global cooling with sea-level regression, and plume-related volcanism (e.g., Korte et al., 2006; Kani et al., 2008; Isozaki, 2009; Wang et al., 2018; Huang et al., 2019; Li et al., 2020). The decrease in the
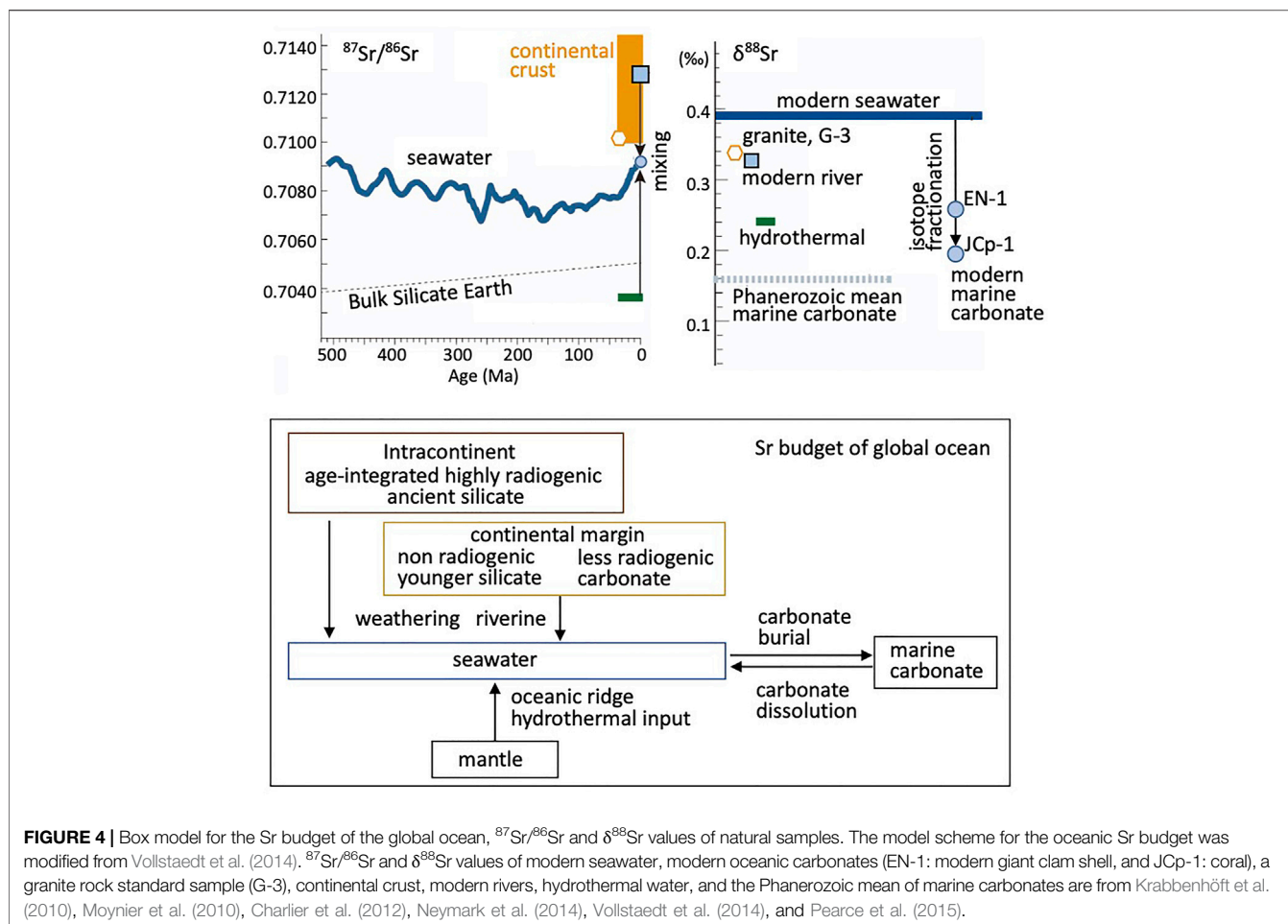
portion of time-integrated highly radiogenic crustal silicate in rivers and then the "continental Sr flux" to the ocean could have been attributed to bias from less radiogenic carbonate and younger silicate on the peripheral side of the continent through the early-middle Permian (**Figure 4**). Given that the hydrothermal flux from the mid-ocean hydrothermal system is relatively constant, a decrease in seawater ^{87}Sr/^{86}Sr values is attributed to the suppression of flux from continental crust *via* the reduction in carbonate/silicate weathering and/or the preservation of weathered products in the interiors of continents far from ocean margins; *vice versa*, an increase in seawater ^{87}Sr/^{86}Sr values is attributed to the accelerated release of continental material into oceans.

Regarding the significant mode change in continental flux from the suppression to the recurrence on a large scale, during the early-middle Permian, a unidirectional decrease in seawater ^{87}Sr/^{86}Sr values occurred (**Figure 2**), probably by the gradual shutdown of riverine transport of weathered material derived from continental crust of the supercontinent Pangea at its maximum size. After reaching the minimum for ca. 5 m.y. in the Capitanian, seawater ^{87}Sr/^{86}Sr values started to increase from the beginning of the Wuchiapingian. The trend decreases again during mid-Wuchiapingian to the end of the Changsingian. The major change in the ^{87}Sr/^{86}Sr trend since the end of the Lopingian is characterized by an unusually high increasing rate. This probably reflected the extremely rapid release of weathered materials derived from continental crust, after their long-term storage in the interior of the continents during the earlier half of the Permian.

In general, tectonics and climate change on a global scale have traditionally been regarded as the main drivers of seawater Sr composition (e.g., Veizer et al., 1999; McArthur et al., 2012). This is because the two processes can considerably change the continental flux of radiogenic Sr to a certain degree. In the following, we briefly review major interpretations and discussions on these two aspects.

PANGEAN TECTONICS

It has been frequently pointed out that the secular changes in Proterozoic-Phanerozoic seawater Sr isotope compositions faithfully reflect changes in configurations of continents over time, particularly the formation and breakup of supercontinents (e.g. Halverson et al., 2007; Condie and Aster, 2013). Pangea's history from its assembly in the Carboniferous to its breakup in the Jurassic apparently coincides not only with the Phanerozoic sea-level changes (Schopf, 1970) but also with the long-term profile of seawater Sr records, which are characterized by a unidirectional decrease during most of the Paleozoic, and, subsequently, a unidirectional increase during the post-Jurassic Mesozoic and Cenozoic (e.g., Veizer et al., 1999). The gathering of various continental blocks could prevent the release of highly radiogenic silicate from the interior of the supercontinent to the ocean by closing intercontinental seaways, and *vice versa*, the post-Pangean opening of the Atlantic Ocean, coupled with the dispersal of continental blocks could elevate the continental flux by creating new passages to oceans.

FIGURE 4 | Box model for the Sr budget of the global ocean, $^{87}Sr/^{86}Sr$ and $\delta^{88}Sr$ values of natural samples. The model scheme for the oceanic Sr budget was modified from Vollstaedt et al. (2014). $^{87}Sr/^{86}Sr$ and $\delta^{88}Sr$ values of modern seawater, modern oceanic carbonates (EN-1: modern giant clam shell, and JCp-1: coral), a granite rock standard sample (G-3), continental crust, modern rivers, hydrothermal water, and the Phanerozoic mean of marine carbonates are from Krabbenhöft et al. (2010), Moynier et al. (2010), Charlier et al. (2012), Neymark et al. (2014), Vollstaedt et al. (2014), and Pearce et al. (2015).

Although the overall picture appears reasonable, it seems difficult to explain the details, such as the Capitanian minimum and subsequent extremely rapid increase after the GLB (Kani et al., 2008). The timing was too early for the main continental breakup, which indeed occurred in the Jurassic, more than 60 m.y. later. The uplifted intracontinental silicate weathering area had grown extensively by continental doming due to mantle plume impingement (Kani et al., 2013) and by the reduced weight of the ice sheets on continents under a warm climate. Some troughs in the seawater $^{87}Sr/^{86}Sr$ curve in the Mesozoic appear to coincide with the emplacement of large igneous provinces (LIPs) (Taylor and Lasaga, 1999; Cohen and Coe 2007; Callegaro et al., 2012; Kristall et al., 2017), which might temporarily contribute to the decline in $^{87}Sr/^{86}Sr$ in seawater. In the Capitanian, submarine hydrothermal activity associated with the opening of Neotethys and the erosion of the Emeishan basaltic rocks might have provided a large flux of nonradiogenic Sr into the oceans (Korte et al., 2006; Huang et al., 2019; Li et al., 2020). Although these apparently contradict with expected constant submarine hydrothermal activity under a stable supercontinent during Permian and increasing continental weathering the Emeishan LIP activity (Henderson et al., 2012), the period of the opening of Neotethys and the period and rate of the erosion of the Emeishan basalts and their quantitative contributions may be worthy considerations as the short-term contributions. After

the Capitanian minimum, the cessation of basaltic volcanism with the decline of hydrothermal activity was suggested (Korte et al., 2006; Wignall et al., 2009). Bagherpour et al. (2018) explained that the temporary decline in seawater $^{87}Sr/^{86}Sr$ during the Wuchiapingian may have reflected an increase in nonradiogenic flux from enhanced continental erosion related to LIP activity. Some minor fluctuations in the whole Phanerozoic curve possibly reflected pulses of nonradiogenic Sr input related to LIP activities.

At present we still need better explanations for shorter-term changes in global seawater Sr profile. Although smaller in magnitude, several pairs of rapid increases/decreases are identified during the Paleozoic, in which the Capitanian minimum is included. These short-term signals superimposed onto the long-term change are likely related to another essential mechanism, which is totally distinct from the overall supercontinent-relevant scenario. In this regard, large-scale sea-level change coupled with the short-term climate change appears promising, on which we will discuss next.

PERMIAN GLOBAL CLIMATE

Climate changes on a global scale may affect considerably the seawater $^{87}Sr/^{86}Sr$ ratio because global cooling/warming can cause sea-level drop/rise and sometimes glaciation/

deglaciation. Sea-level change and continental ice coverage are critical to continental flux of radiogenic Sr into the oceans, whereas nonradiogenic mid-oceanic ridge flux is not related to climate change. Global cooling may cause sea-level to decrease, which can drive more surface exposure of less radiogenic peripheral continental crusts to enhance less radiogenic flux to ocean. Furthermore, when global cooling involves major glaciation, the ice coverage over extensive intracontinental crusts may suppress more effectively the highly radiogenic continental Sr flux.

The late Paleozoic ice age (LPIA) was identified on the basis of glacial deposits formed at high to mid-paleolatitudes (e.g., Fielding et al., 2008). Although intermittently truncated by short-lived deglaciations, the glacial condition of the LPIA essentially continued for over 50 m.y., i.e., from the Early Pennsylvanian (late Carboniferous) (~320 Ma) to the late Wuchiapingian (ca. 255 Ma) (Montañez and Poulsen, 2013; Frank et al., 2015). At the beginning of the early Cisuralian (early Permian), seawater Sr isotope values started to decrease rapidly, in good accordance with the apex timing of the LPIA with extensive continental glaciation (**Figure 2**). On the other hand, the onset of the Capitanian Sr minimum was during a cold climate with the lowest Phanerozoic sea level, and it continued until the GLB, which roughly corresponded to the termination, rather than in the middle, of the LPIA (**Figure 2**). As to the coeval global cooling/sea-level decrease and Sr isotope minimum, a similar observation was confirmed also for the end-Ordovician timing (Isozaki and Servais, 2018).

In response to a global cooling in the interval, aridity and the post-main Gondwanan glaciation were presumed as possible causes of the decreasing of $^{87}Sr/^{86}Sr$ (Korte et al., 2006; Henderson et al., 2012), rather than local/regional tectonism. In general, glaciation is regarded as an effective agent to increase continental weathering/erosion. For the Capitanian case during the assembly of Pangea, however, the expansion of continental glaciers might have suppressed continental weathering. Kani et al. (2013) explained the decrease in $^{87}Sr/^{86}Sr$ had been derived possibly from the regional ice cover over vast continents under a cool climate. In contrast, as to the increase in $^{87}Sr/^{86}Sr$ during the end of the Lopingian to Early Triassic, the warmer climate associated with sea-level rise might have enhanced the weathering of older intracontinental silicate-dominant crustal rocks, reducing the weathering of younger rocks along ocean margins. The transient increase in $^{87}Sr/^{86}Sr$ at the beginning of the Lopingian likewise possibly resulted from a short-lived warmer climate (Chen et al., 2013). Currently popular scenarios prefer the rapid continental weathering by assuming a global warming triggered by the vast CO_2 emission from the Emeishan LIP volcanism (Henderson et al., 2012), humidification (Korte et al., 2006; Wignall et al., 2009), acid rain (Huang et al., 2008; Song et al., 2015), and resultant loss of land vegetation. Nevertheless, the emerging $\delta^{88}Sr$ data, as introduced in the following section, provide an alternate explanation.

UTILITY OF δ^{88}SR ISOTOPIC SYSTEM

Stable Sr isotope $\{\delta^{88}Sr = [(^{88}Sr/^{86}Sr)_{carbonate}/(^{88}Sr/^{86}Sr)_{standard} - 1] \times 10^3\}$ has been recently recognized as a useful proxy for

monitoring past burial/dissolution of oceanic carbonates (Vollstaedt et al., 2014). The $\delta^{88}Sr$ value of marine carbonate is lighter than that of coeval seawater because carbonate preferentially incorporates lighter ^{86}Sr (**Figure 4**, e.g., Bohm et al., 2012). As confirmed in modern oceans, the degree of burial/dissolution of oceanic carbonate is essential to determine $\delta^{88}Sr$ value of seawater. (Krabbenhöft et al., 2010; Vollstaedt et al., 2014). In general, the rate of preservation/dissolution of oceanic carbonate is attributed to environmental changes, such as seawater temperature, pH, and sea-level change (Riebesell et al., 1993; Knoll et al., 1996; Woods et al., 1999; Payne et al., 2010). During sea-level low stands, in particular, the regional exposure of ancient marine carbonates along continental shelf margins may increase carbonate-derived Sr flux (Stoll and Schrag, 1998; Krabbenhöft et al., 2010), which is characterized by low $\delta^{88}Sr$ (Vollstaedt et al., 2014).

To date, $\delta^{88}Sr$ analysis for ancient marine carbonates has not yet covered the entire Paleozoic (Vollstaedt et al., 2014; **Figure 1**). As to the Permian (Vollstaedt et al., 2014; **Figure 1**), nevertheless, the secular trend of seawater $\delta^{88}Sr$ was preliminarily shown, in which $\delta^{88}Sr$ values started to decrease in the early Permian and kept decreasing till the end of the Capitanian when the lowest value of the Phanerozoic was marked. The minimum of $\delta^{88}Sr$ values strictly during the Capitanian essentially suggest the unique dominance of carbonate weathering/erosion. The carbonate dissolution and associated discharge of less radiogenic Sr likely occurred on continental margins with ample archives of past carbonates, mostly along the Tethyan and low-latitude Panthalassan peripheries during the Permian.

In the Capitanian, the carbonate production declined globally in high latitudes, with the significant shrinkage of reef ecosystems (e.g., Beauchamp and Grasby, 2012; Blomeier et al., 2013). For the cause of this temporary shutdown of bio-carbonate factory, possible candidates include global cooling, anoxia, or acidification (Bond et al., 2015). Temperature drop in seawater, in particular, promotes the dissolution of carbonate, as the increase of pCO_2 in seawater leads higher solubility (Freeman and Hays, 1992) to move the carbonate lysocline to shallower levels, and to limit consequently the depositional area on seafloor for carbonates.

The overall correlation between $\delta^{88}Sr$ and $^{87}Sr/^{86}Sr$ throughout the Phanerozoic has not been examined owing to the incomplete dataset; however, the secular change in seawater $\delta^{88}Sr$ did not apparently synchronize with that of $^{87}Sr/^{86}Sr$ (Vollstaedt et al., 2014; **Figure 1**); i.e., these two curves often deviate from each other with remarkable off-sets in timing of inflection points. Nevertheless, for the Middle-Late Permian interval, an intimate correlation is observed between $\delta^{88}Sr$ and $^{87}Sr/^{86}Sr$ (**Figure 1**); i.e., the shape of the $\delta^{88}Sr$ trend during the Permian in the vertex of the parabola centered in the Capitanian is almost identical to that of coeval $^{87}Sr/^{86}Sr$. The synchronized decreases in the seawater $^{87}Sr/^{86}Sr$ and $\delta^{88}Sr$ values are likely caused by the elevated input of less radiogenic and ^{86}Sr-enriched carbonate-derived flux through intense weathering/dissolution along continental margins. Although the causes of changes in preservation/dissolution were differently each changes in $\delta^{88}Sr$ curve through Phanerozoic, the dual isotopic systems i.e., $\delta^{88}Sr$

and $^{87}Sr/^{86}Sr$ provide a further information to understand global Sr budget changes. By analyzing secular changes in seawater $\delta^{88}Sr$, we can reconstruct the history of preservation/dissolution of carbonates at continental margin as a global average.

Vollstaedt et al. (2014) also pointed out that the long-term trends of $\delta^{44/40}Ca$ and $\delta^{88}Sr$ resemble each other throughout the Phanerozoic, which reflect variations in carbonate fluxes in global Ca and Sr cycles. The changes in $\delta^{88}Sr$ likely synchronized with carbon isotope excursions, as well as that of Ca stable isotope, because the carbon and calcium cycles are generally coupled *via* $CaCO_3$ preservation/dissolution processes. The post-Kamura negative shift in $\delta^{13}C$ in the Capitanian may have reflected an enhanced marine carbonate dissolution. As to the PTB, the $\delta^{13}C$ negative shift from +3 to −1 permil (Korte and Kozur, 2010) and Ca isotope negative shift were explained by the dissolution of ^{13}C-depleted carbonate, which was triggered likely by oceanic acidification (Hinojosa et al., 2012). The expected co-variation of $\delta^{44/40}Ca$ and $\delta^{88}Sr$ in seawater is not clear for the GLB interval. The $\delta^{88}Sr$ may have been dependent only on changes in carbonate flux (Vollstaedt et al., 2014), whereas $\delta^{44/40}Ca$ was influenced probably by different fractionation factors between calcite and aragonite (Farkas et al., 2007; Blattler et al., 2012). There is no $\delta^{13}C$ negative excursion nor consistent pattern in $\delta^{44/40}Ca$ confirmed in three distinct sections across GLB in the southern Tethyan domain (Penglaitan and Chaotian section in China, and in Köserelik Tepe in Turkey), which may reflect local effects or diagenetic alteration (Jost et al., 2014). For establishing a quantitative model, it is required that investigations of the magnitude and timing of variations of $\delta^{88}Sr$ and other geochemical proxies as indicators of the ocean chemical condition during the Capitanian-Wuchiapingian interval, on continuous sequences of carbonates without local effects or alteration.

CAPITANIAN ENVIRONMENTAL CHANGES WITH EXTINCTION

Besides the above-discussed beacon in the Sr isotope episode, other geological records, such as the lowest sea-level of the Phanerozoic (Haq and Schutter, 2008; Kofukuda et al., 2014), C-isotope anomaly called the Kamura event (Isozaki et al., 2007; Isozaki et al., 2011), and the major geomagnetic excursion called the Illawara Reversal (Isozaki, 2009a), altogether indicate that major global environmental changes surely appeared in the Capitanian and across the GLB. The uniqueness of this interval has been focused also in view of biodiversity crisis with the Capitanian extinction (Jin et al., 1994, Jin et al., 2006b; Stanley and Yang, 1994; Bambach, 2002; Isozaki, 2009; Bond et al., 2010 etc.), which is rated high in the ranking of the extinction magnitude (McGhee and Mukhopadhyay, 2013; Stanley, 2016). The main cause and processes of this global scale episode were not yet fully revealed, although various possible scenarios were proposed; e.g., the Emeishan Trap volcanism (Chung et al., 1998; Ali et al., 2002; Wignall et al., 2009), the onset of global anoxia (Isozaki, 1997; Saitoh et al.,

2014); non-bolide extraterrestrial effect (Isozaki, 2019). The coeval unique signals in C, S, and N isotope records across the GLB (e.g., Isozaki et al., 2007; Saitoh et al., 2013; Yan et al., 2013; Bond et al., 2015; Zhang et al., 2015; Maruoka and Isozaki, 2020) further imply strong links to the major environmental changes with extinction.

As to the Sr behavior in the Permian ocean, sea-level change and relevant development/retreat of reef carbonates appear more critical than the rest. The Permian reef ecosystems were severely destructed during the Capitanian, and their recovery was extremely slow afterwards until the late Wuchiapingian (e.g., Weidlich, 2002). In addition to the low-latitude reef complexes, high-latitude carbonates also disappeared quickly, e.g. in Greenland and Spitsbergen, during the Capitanian (e.g., Beauchamp and Grasby, 2012; Blomeier et al., 2013). This profound collapse of carbonate factory was likely caused by the claimed global cooling associated with the remarkable sea-level drop (Haq and Schutter, 2008; Kofukuda et al., 2014), which is supported also by the selective extinction of warm-water adapted biota and the end of gigantism among symbiotic biota (Isozaki and Aljinovic, 2009; Feng et al., 2020), and also the migration of mid-latitude fauna to low latitude domains (Shen and Shi, 2002).

It seems difficult to specify any direct cause-effect relationship between the nonbiological Sr episodes and extinction; however, both phenomena were caused by a large-scale agent of global context that appeared during the Capitanian. The ultimate driver of such global change is not yet identified; nevertheless, global cooling and carbonate dissolution appear as the most significant explanation for the Sr records and other lines of geological evidence at present. The seawater $^{87}Sr/^{86}Sr$ changes, the minimum or the maximum, seem to coincide with several extinction events, e.g., the end-Ordovician, the end-Guadalupian, and the end-Permian (**Figure 1**). Recently, various similarities were recognized between two major extinction-related episodes in the Paleozoic; i.e., the Hirnantian (end-Ordovician) and Capitanian (end-Permian) events, because both episodes commonly recorded the preferential removal of sessile biota in the tropics, global sea-level drop, negative excursion of carbon isotopes, and end of long-term geomagnetic polarity interval (Isozaki and Servais, 2018; Isozaki, 2019). This may promote further research on other cooling-relevant extinction events and coeval changes in Sr isotope signatures in global oceans.

SUMMARY

The "Capitanian minimum" episode of Sr isotope records is reviewed, particularly in terms of dual Sr isotopic systems; i.e., $^{87}Sr/^{86}Sr$ ratio and $\delta^{88}Sr$ value. The long-term trend of the Paleozoic seawater $^{87}Sr/^{86}Sr$ was punctuated by the Capitanian minimum at the end of the Guadalupian (Permian). The lowest value of seawater $^{87}Sr/^{86}Sr$ (0.7068) in the Capitanian and subsequent rapid increase at an unusually high rate likely originated from a significant

change in continental flux with highly radiogenic Sr with respect to relatively stable hydrothermal flux from MORs. The assembly of the supercontinent Pangea and subsequent mantle plume-induced breakup were responsible for the overall secular change throughout the Phanerozoic; nonetheless, short-term fluctuations were superimposed by global climate changes. The unidirectional decrease in Sr isotope values during the early-middle Permian and the Capitanian minimum was driven by the suppression of continental flux with time-integrated highly radiogenic silicates and also by the extensive dissolution of carbonates with less radiogenic Sr along continental margins. During the existence of Pangea, a cold climate appeared to develop extensive ice covers over continents, as well as the lowest sea-level. In contrast, the extremely rapid increase in Sr isotope values during the end of the Lopingian-Early Triassic was induced by global warming, during which all processes worked in the opposite manner. Major changes in the Capitanian surface environments, including the significant sea-level drop, system disturbance in Sr and other isotope, decline in carbonate formation, and large-scale biodiversity crisis called the end-Guadalupian extinction, were all consequences of a rare and large-scale agent that appeared not only during the Capitanian but also in other cooling/extinction relevant timings.

REFERENCES

Ali, J. R., Thompson, G. M., Song, X., and Wang, Y. (2002). Emeishan Basalts (SW China) and the 'end-Guadalupian' Crisis: Magnetobiostratigraphic Constraints. *J. Geol. Soc.* 159, 21–29. doi:10.1144/0016-764901086

Allègre, C. J., Louvat, P., Gaillardet, J., Meynadier, L., Rad, S., and Capmas, F. (2010). The Fundamental Role of Island Arc Weathering in the Oceanic Sr Isotope Budget. *Earth Planet. Sci. Lett.* 292 (1–2), 51–56. doi:10.1016/j.epsl.2010.01.019

Bagherpour, B., Bucher, H., Yuan, D.-x., Leu, M., Zhang, C., and Shen, S.-Z. (2018). Early Wuchiapingian (Lopingian, Late Permian) Drowning Event in the South China Block Suggests a Late Eruptive Phase of Emeishan Large Igneous Province. *Glob. Planet. Change* 169, 119–132. doi:10.1016/j.gloplacha.2018.07.013

Bambach, R. K., Knoll, A. H., and Sepkoski, J. J., Jr. (2002). Anatomical and Ecological Constraints on Phanerozoic Animal Diversity in the marine Realm. *Proc. Natl. Acad. Sci.* 99 (10), 6854–6859. doi:10.1073/pnas.092150999

Banner, J. L. (2004). Radiogenic Isotopes: Systematics and Applications to Earth Surface Processes and Chemical Stratigraphy. *Earth-Science Rev.* 65, 141–194. doi:10.1016/s0012-8252(03)00086-2

Beauchamp, B., and Grasby, S. E. (2012). Permian Lysocline Shoaling and Ocean Acidification along NW Pangea Led to Carbonate Eradication and Chert Expansion. *Palaeogeogr. Palaeoclimatol. Palaeoecol.* 350-352, 73–90. doi:10.1016/j.palaeo.2012.06.014

Blättler, C. L., Henderson, G. M., and Jenkyns, H. C. (2012). Explaining the Phanerozoic Ca Isotope History of Seawater. *Geology* 40, 843–846. doi:10.1130/G33191.1

Blomeier, D. P. G., Dustira, A. M., Forke, H., and Scheibner, C. (2013). Facies Analysis and Depositional Environments of a Storm-Dominated, Temperate to Cold, Mixed Siliceouscarbonate Ramp: the Permian Kapp Starostin Formation in NE Svalbard. *Norwegian J. Geology.* 93, 75–98.

Bodin, S., Meissner, P., Janssen, N. M. M., Steuber, T., and Mutterlose, J. (2015). Large Igneous Provinces and Organic Carbon Burial: Controls on Global Temperature and continental Weathering during the Early Cretaceous. *Glob. Planet. Change* 133, 238–253. doi:10.1016/j.gloplacha.2015.09.001

AUTHOR CONTRIBUTIONS

FUNDING

ACKNOWLEDGMENTS

SUPPLEMENTARY MATERIAL

The Supplementary Material for this article can be found online at: https://www.frontiersin.org/articles/10.3389/feart.2021.662581/full#supplementary-material

Böhm, F., Eisenhauer, A., Tang, J., Dietzel, M., Krabbenhöft, A., Kisakürek, B., et al. (2012). Strontium Isotope Fractionation of Planktic Foraminifera and Inorganic Calcite. *Geochimica et Cosmochimica Acta* 93, 300–314. doi:10.1016/j.gca.2012.04.038

Bond, D. P. G., Hilton, J., Wignall, P. B., Ali, J. R., Stevens, L. G., Sun, Y. D., et al. (2010). The Middle Permian (Capitanian) Mass Extinction on Land and in the Oceans. *Earth-Science Rev.* 102 (1–2), 100–116. doi:10.1016/j.earscirev.2010.07.004

Bond, D. P. G., Wignall, P. B., Joachimski, M. M., Sun, Y. D., Savov, I., and Grasby, S. E. (2015). An Abrupt Extinction in the Middle Permian (Capitanian) of the Boreal Realm (Spitsbergen) and its Link to Anoxia and Acidification. *Geol. Soc. America Bull.* 127 (9–10), 1411–1421. doi:10.1130/b31216.1

Burke, W. H., Denison, R. E., Hetherington, E. A., Koepnick, R. B., Nelson, H. F., and Otto, J. B. (1982). Variation of Seawater 87Sr/86Sr throughout Phanerozoic Time. *Geol* 10, 516–519. doi:10.1130/0091-7613(1982)10<516:vosstp>2.0.co;2

Callegaro, S., Rigo, M., Chiaradia, M., and Marzoli, A. (2012). Latest Triassic marine Sr Isotopic Variations, Possible Causes and Implications. *Terra Nova* 24, 130–135. doi:10.1111/j.1365-3121.2011.01046.x

Charlier, B. L. A., Nowell, G. M., Parkinson, I. J., Kelley, S. P., Pearson, D. G., and Burton, K. W. (2012). High Temperature Strontium Stable Isotope Behaviour in the Early Solar System and Planetary Bodies. *Earth Planet. Sci. Lett.* 329-330, 31–40. doi:10.1016/j.epsl.2012.02.008

Chen, B., Joachimski, M. M., Shen, S.-z., Lambert, L. L., Lai, X.-l., Wang, X.-d., et al. (2013). Permian Ice Volume and Palaeoclimate History: Oxygen Isotope Proxies Revisited. *Gondwana Res.* 24, 77–89. doi:10.1016/j.gr.2012.07.007

Chung, S.-L., Jahn, B.-m., Genyao, W., Lo, C.-H., and Bolin, C. (1998). "The Emeishan Flood basalt in SW China: A Mantle Plume Initiation Model and its Connection with continental Breakup and Mass Extinction at the Permian-Triassic Boundary," in *Mantle Dynamics and Plate Interactions in East Asia American Geophysical Union, Geodynamics Series*. Editors M. F. J. Flower, S. Chung, C. Lo, and T. Lee (Washington, D.C.: American Geophysical Union), 47–58. doi:10.1029/GD027p0047

Cohen, A. S., and Coe, A. L. (2007). The Impact of the Central Atlantic Magmatic Province on Climate and on the Sr- and Os-Isotope Evolution of Seawater. *Palaeogeogr. Palaeoclimatol. Palaeoecol.* 244, 374–390. doi:10.1016/j.palaeo.2006.06.036

Condie, K. C., and Aster, R. C. (2013). Refinement of the Supercontinent Cycle with Hf, Nd and Sr Isotopes. *Geosci. Front.* 4, 667. doi:10.1016/j.gsf.2013.06.001

Denison, R. E., Koepnick, R. B., Burke, W. H., Hetherington, E. A., and Fletcher, A. (1994). Construction of the Mississippian, Pennsylvanian and Permian Seawater ^{87}Sr/^{86}Sr Curve. *Chem. Geology.* 112 (1–2), 145–167. doi:10.1016/0009-2541(94)90111-2

DePaolo, D. J., and Ingram, B. L. (1985). High-resolution Stratigraphy with Strontium Isotopes. *Science* 227, 938–941. doi:10.1126/science.227.4689.938

Dera, G., Brigaud, B., Monna, F., Laffont, R., Pucéat, E., Deconinck, J.-F., et al. (2011). Climatic Ups and downs in a Disturbed Jurassic World. *Bull. Geol. Soc. Am.* 39 (3), 215–218. doi:10.1130/g31579.1

Farkas, J., Bohm, F., Wallmann, K., Blenkinsop, J., Eisenhauer, A., van Geldern, R., et al. (2007). Calcium Isotope Record of Phanerozoic Oceans: Implications for Chemical Evolution of Seawater and its Causative Mechanisms. *Geochim. Cosmochim. Acta* 71, 5117–5134. doi:10.1016/j.gca.2007.09.004

Feng, Y., Song, H., and Bond, D. P. G. (2020). Size Variations in Foraminifers from the Early Permian to the Late Triassic: Implications for the Guadalupian–Lopingian and the Permian–Triassic Mass Extinctions. *Paleobiology* 46(4) (2020), 511–532. doi:10.1017/pab.2020.37

Fielding, C. R., Frank, T. D., Birgenheier, L. P., Rygel, M. C., Jones, A. T., and Roberts, J. (2008). Stratigraphic Imprint of the Late Palaeozoic Ice Age in Eastern Australia: A Record of Alternating Glacial and Nonglacial Climate Regime. *J. Geol. Soc.* 165, 129–140. doi:10.1144/0016-76492007-036

Frank, T. D., Shultis, A. I., and Fielding, C. R. (2015). Acme and Demise of the Late Palaeozoic Ice Age: A View from the southeastern Margin of Gondwana. *Palaeogeogr. Palaeoclimatol. Palaeoecol.* 418, 176–192. doi:10.1016/j.palaeo.2014.11.016

Freeman, K. H., and Hayes, J. M. (1992). Fractionation of Carbon Isotopes by Phytoplankton and Estimates of Ancient CO2levels. *Glob. Biogeochem. Cycles* 6, 185–198. doi:10.1029/92gb00190

Friedrich, O., Norris, R. D., and Erbacher, J. (2012). Evolution of Middle to Late Cretaceous Oceans-A 55 m.Y. Record of Earth's Temperature and Carbon Cycle. *no* 40, 107–110. doi:10.1130/G32701.1

Glenister, B. F., Boyd, D. W., Furnish, W. M., Grant, R. E., Harris, M. T., Kozur, H., et al. (1992). The Guadalupian: Proposed International Standard for a Middle Permian Series. *Int. Geology. Rev.* 34 (9), 857–888. doi:10.1080/00206819209465642

Goldstein, S. J., and Jacobsen, S. B. (1987). The Nd and Sr Isotopic Systematics of River-Water Dissolved Material: Implications for the Sources of Nd and Sr in Seawater. *Chem. Geology. Isotope Geosci. section* 66, 245–272. doi:10.1016/0168-9622(87)90045-5

Gradstein, F. M., Ogg, J. G., Schmitz, M., and Ogg, G. (2012). *The Geologic Time Scale 2012.* Amsterdam: Elsevier, 1127.

Halverson, G. P., DudásÖ., F. Ö., Maloof, A. C., and Bowring, S. A. (2007). Evolution of the 87Sr/86Sr Composition of Neoproterozoic Seawater. *Palaeogeogr. Palaeoclimatol. Palaeoecol.* 256, 103–129. doi:10.1016/j.palaeo.2007.02.028

Haq, B. U., and Schutter, S. R. (2008). A Chronology of Paleozoic Sea-Level Changes. *Science* 322, 64–68. doi:10.1126/science.1161648

Henderson, C. M., Davydov and, V. I., Wardlaw, B. R., Gradstein, F. M., and Hammer, O. (2012). "The Permian Period," in *The Geological Time Scale 2012.* Editors F. M. Gradstein, J. G. Ogg, M. D. Schmitz, and G. M. Ogg (Amsterdam: Elsever), 653–679. doi:10.1016/b978-0-444-59425-9.00024-x

Henderson, C. M., and Mei, S. L. (2007). Geographical Clines in Permian and Lower Triassic Gondolellids and its Role in Taxonomy. *Palaeoworld* 16, 190e201. doi:10.1016/j.palwor.2007.05.014

Hess, J., Bender, M. L., and Schilling, J.-G. (1986). Evolution of the Ratio of Strontium-87 to Strontium-86 in Seawater from Cretaceous to Present. *Science* 231, 979–984. doi:10.1126/science.231.4741.979

Hess, J., Stott, L. D., Bender, M. L., Kennett, J. P., and Schilling, J.-G. (1989). The Oligocene marine Microfossil Record: Age Assessments Using Strontium Isotopes. *Paleoceanography* 4, 655–679. doi:10.1029/PA004i006p00655

Hinojosa, J. L., Brown, S. T., Chen, J., DePaolo, D. J., Paytan, A., Shen, S.-z., et al. (2012). Evidence for End-Permian Ocean Acidification from Calcium Isotopes in Biogenic Apatite. *Geology* 40 (8), 743–746. doi:10.1130/G33048.1

Holland, H. D. (2003). The Geologic History of Seawater. *Treatise Geochem.* 6, 583–625.

Huang, H., Hou, M., Qing, H., Zhou, L., Yang, J., Du, Y., et al. (2019). The Contribution of the Emeishan Large Igneous Province to the Strontium Isotope Evolution of the Capitanian Seawater. *Int. Geology. Rev.* 61 (15), 1927–1939. doi:10.1080/00206814.2019.1571448

Huang, S., Qing, H., Huang, P., Hu, Z., Wang, Q., Zou, M., et al. (2008). Evolution of Strontium Isotopic Composition of Seawater from Late Permian to Early Triassic Based on Study of marine Carbonates, Zhongliang Mountain, Chongqing, China. *Sci. China Ser. D-earth Sci.* 51, 528–539. doi:10.1007/s11430-008-0034-3

Isozaki, Y., and Aljinovic, D. (2009). End-Guadalupian Extinction of the Permian Gigantic Bivalve Alatoconchidae: End of Gigantism in Tropical Seas by Cooling. *Palaeogeogr. Palaeoclimatol. Palaeoecol.* 284 (1–2), 11–21. doi:10.1016/j.palaeo.2009.08.022

Isozaki, Y., Aljinović, D., and Kawahata, H. (2011). The Guadalupian (Permian) Kamura Event in European Tethys. *Palaeogeogr. Palaeoclimatol. Palaeoecol.* 308, 12–21. doi:10.1016/j.palaeo.2010.09.034

Isozaki, Y. (2019). "End-Paleozoic Mass Extinction: Hierarchy of Causes and a New Cosmoclimatological Perspective for the Largest Crisis," in *Astrobiology.* Editors A. Yamagishi, T. Kakegawa, and T. Usui. (Singapore: Springer), 273–301. doi:10.1007/978-981-13-3639-3_18:

Isozaki, Y. (2009). Integrated "plume winter" Scenario for the Double-Phased Extinction during the Paleozoic-Mesozoic Transition: The G-LB and P-TB Events from a Panthalassan Perspective. *J. Asian Earth Sci.* 36, 459–480. doi:10.1016/j.jseaes.2009.05.006

Isozaki, Y., Kawahata, H., and Ota, A. (2007). A Unique Carbon Isotope Record across the Guadalupian-Lopingian (Middle-Upper Permian) Boundary in Mid-oceanic Paleo-Atoll Carbonates: The High-Productivity "Kamura Event" and its Collapse in Panthalassa. *Glob. Planet. Change* 55, 21–38. doi:10.1016/j.gloplacha.2006.06.006

Isozaki, Y., Maruyama, S., and Furuoka, F. (1990). Accreted Oceanic Materials in Japan. *Tectonophysics* 181, 179–205. doi:10.1016/0040-1951(90)90016-2

Isozaki, Y., Nakahata, H., Zakharov, Y. D., Popov, A. M., Sakata, S., and Hirata, T. (2017). Greater South China Extended to the Khanka Block: Detrital Zircon Geochronology of Middle-Upper Paleozoic Sandstones in Primorye, Far East Russia. *J. Asian Earth Sci.* 145, 565–575. doi:10.1016/j.jseaes.2017.06.027

Isozaki, Y., and Ota, A. (2001). Middle-Upper Permian (Maokouan-Wuchiapingian) Boundary in Mid-oceanic Paleo-Atoll limestone of Kamura and Akasaka, Japan. *Proc. Jpn. Acad. Ser. B: Phys. Biol. Sci.* 77, 104–109. doi:10.2183/pjab.77.104

Isozaki, Y. (1997). Permo-Triassic Boundary Superanoxia and Stratified Superocean: Records from Lost Deep Sea. *Science* 276, 235–238. doi:10.1126/science.276.5310.235

Isozaki, Y., and Servais, T. (2018). The Hirnantian (Late Ordovician) and End-Guadalupian (Middle Permian) Mass-Extinction Events Compared. *Lethaia* 51, 173–186. doi:10.1111/let.12252

Jahren, G. J., and au, A. H. (2008). Methane Release from Igneous Intrusion of Coal during Late Permian Extinction Events. *J. Geology.* 116, 1–20. doi:10.1086/524120

Jin, Y. G., Shen, S. Z., Henderson, C. M., Wang, X. D., Wang, W., Wang, Y., et al. (2006a). The Global Stratotype Section and Point (GSSP) for the Boundary between the Capitanian and Wuchiapingian Stage (Permian). *Episodes* 29, 253e262. doi:10.18814/epiiugs/2006/v29i4/003

Jin, Y. G., Wang, Y., Henderson, C. M., Wardlaw, B. R., Shen, S. Z., and Cao, C. Q. (2006b). The GSSP for the Base of the Changhsingian Stage (Upper Permian). *Episodes* 29, 175e182. doi:10.18814/epiiugs/2006/v29i3/003

Jin, Y. G., Zhang, J., and Shang, Q. H. (1994). Two Phases of End-Permian Mass Extinction. *Can. Soc. Pet. Geologists Memoir* 17, 813–822.

Jost, A. B., Mundil, R., He, B., Brown, S. T., Altiner, D., Sun, Y., et al. (2014). Constraining the Cause of the End-Guadalupian Extinction with Coupled Records of Carbon and Calcium Isotopes. *Earth Planet. Sci. Lett.* 396, 201–212. doi:10.1016/j.epsl.2014.04.014

Kaiho, K., Chen, Z. Q., Ohashi,Arinobu, T. T., Sawada, K., and Cramer, B. S. (2005). A Negative Carbon Isotope Anomaly Associated Withth Eearliest Lopingian (Late Permian) Mass Extinction. *Palaeogeogr. Palaeoclimatol. Palaeoecol.* 223, 172–180. doi:10.1016/j.palaeo.2005.04.013

Kani, T., Fukui, M., Isozaki, Y., and Nohda, S. (2008). The Paleozoic Minimum of 87Sr/86Sr Ratio in the Capitanian (Permian) Mid-oceanic Carbonates: A

Critical Turning point in the Late Paleozoic. *J. Asian Earth Sci.* 32 (1), 22–33. doi:10.1016/j.jseaes.2007.10.007

Kani, T., Hisanabe, C., and Isozaki, Y. (2013). The Capitanian (Permian) Minimum of 87Sr/86Sr Ratio in the Mid-panthalassan Paleo-Atoll Carbonates and its Demise by the Deglaciation and continental Doming. *Gondwana Res.* 24 (1), 212–221. doi:10.1016/j.gr.2012.08.025

Kani, T., Isozaki, Y., Hayashi, R., Zakharov, Y., and Popov, A. (2018). Middle Permian (Capitanian) Seawater 87 Sr/ 86 Sr Minimum Coincided with Disappearance of Tropical Biota and Reef Collapse in NE Japan and Primorye (Far East Russia). *Palaeogeogr. Palaeoclimatol. Palaeoecol.* 499, 13–21. doi:10.1016/j.palaeo.2018.03.033

Kasuya, A., Isozaki, Y., and Igo, H. (2012). Constraining Paleo-Latitude of a Biogeographic Boundary in Mid-panthalassa: Fusuline Province Shift on the Late Guadalupian (Permian) Migrating Seamount. *Gondwana Res.* 21, 611–623. doi:10.1016/j.gr.2011.06.001

Kawamura, T., and Machiyama, H. (1995). A Late Permian Coral Reef Complex, South Kitakami Terrane, Japan. *Sediment. Geology.* 99, 135–150. doi:10.1016/0037-0738(95)00040-f

Knoll, A. H., Bambach, R. K., Canfield, D. E., and Grotzinger, J. P. (1996). Comparative Earth History and Late Permian Mass Extinction. *Science* 273, 452–457. doi:10.1126/science.273.5274.452

Kofukuda, D., Isozaki, Y., and Igo, H. (2014). A Remarkable Sea-Level Drop and Relevant Biotic Responses across the Guadalupian-Lopingian (Permian) Boundary in Low-Latitude Mid-panthalassa: Irreversible Changes Recorded in Accreted Paleo-Atoll Limestones in Akasaka and Ishiyama, Japan. *J. Asian Earth Sci.* 82, 47–65. doi:10.1016/j.jseaes.2013.12.010

Korte, C., Jasper, T., Kozur, H. W., and Veizer, J. (2006). ^{87}Sr/^{86}Sr Record of Permian Seawater. *Palaeogeogr. Palaeoclimatol. Palaeoecol.* 240 (1–2), 89–107. doi:10.1016/j.palaeo.2006.03.047

Korte, C., Kozur, H. W., Bruckschen, P., and Veizer, J. (2003). Strontium Isotope Evolution of Late Permian and Triassic Seawater. *Geochimica et Cosmochimica Acta* 67 (1), 47–62. doi:10.1016/s0016-7037(02)01035-9

Korte, C., and Kozur, H. W. (2010). Carbon-isotope Stratigraphy across the Permian-Triassic Boundary: a Review. *J. Asian Earth Sci.* 39, 215–235. doi:10.1016/j.jseaes.2010.01.005

Korte, C., Kozur, H. W., Joachimski, M. M., Strauss, H., Veizer, J., and Schark, L. (2004). Carbon, Sulfur, Oxygen and Strontium Isotope Records, Organic Geochemistry and Biostratigraphy across the Permian/Triassic Boundary in Abadeh, Iran. *Int. J. Earth Sci.* 93, 565–581. doi:10.1007/s00531-004-0406-7

Korte, C., and Ullmann, C. V. (2016). Permian Strontium Isotope Stratigraphy. *Geol. Soc. Lond. Spec. Publications* 450 (1), 105–118. doi:10.1144/sp450.5

Kossovaya, O. L., and Kropatcheva, G. S. (2013). "Extinction of Guadalupian Rugose Corals: an Example of Biotic Response to the Kamura Event (Southern Primorye, Russia)," in , *Palaeozoic Climate Cycles: Their Evolutionary and Sedimentological Impact*, London: Geological Society, 376, 407–429. doi:10.1144/sp376.13

Krabbenhöft, A., Eisenhauer, A., Böhm, F., Vollstaedt, H., Fietzke, J., Liebetrau, V., et al. (2010). Constraining the marine Strontium Budget with Natural Strontium Isotope Fractionations (87Sr/86Sr∗, δ88/86Sr) of Carbonates, Hydrothermal Solutions and River Waters. *Geochimica et Cosmochimica Acta* 74, 4097–4109. doi:10.1016/j.gca.2010.04.009

Kristall, B., Jacobson, A. D., and Hurtgen, M. T. (2017). Modeling the Paleo-Seawater Radiogenic Strontium Isotope Record: A Case Study of the Late Jurassic-Early Cretaceous. *Palaeogeogr. Palaeoclimatol. Palaeoecol.* 472, 163–176. doi:10.1016/j.palaeo.2017.01.048

Li, Q., Azmi, K., Yang, S., Xu, S.-L., Yang, D., Zhang, X.-H., et al. (2020). *Early–middle Permian Strontium Isotope Stratigraphy Marine Carbonates Northern Marginal Areas South. China: Controlling Factors Implications Geol. Jour.* 2020, 1–15. doi:10.1002/gj.4010

Li, Q., Yang, S., Azmy, K., Chen, H., Hou, M., Wang, Z., et al. (2021). Strontium Isotope Evolution of Middle Permian Seawater in the Sichuan Basin, South China: Possible Causes and Implications. *Palaeogeogr. Palaeoclimatol. Palaeoecol.* 565, 110188. doi:10.1016/j.palaeo.2020.110188

Liu, X.-c., Wang, W., Shen, S.-z., Gorgij, M. N., Ye, F.-c., Zhang, Y.-c., et al. (2013). Late Guadalupian to Lopingian (Permian) Carbon and Strontium Isotopic Chemostratigraphy in the Abadeh Section, central Iran. *Gondwana Res.* 24 (1), 222–232. doi:10.1016/j.gr.2012.10.012

Lucas, S. (2021). Nonmarine Mass Extinctions. *Paleontological Res.* 25. doi:10.2517/2021PR004

Martin, E. E., and Macdougall, J. D. (1995). Sr and Nd Isotopes at the Prmian/triassic Boundary: A Record of Climate Change. *Chem. Geology.* 125 (1–2), 73–99. doi:10.1016/0009-2541(95)00081-v

Metcalfe, I., Crowley, J. L., Nicoll, R. S., and Schmitz, M. (2015). High-precision U-Pb CA-TIMS Calibration of Middle Permian to Lower Triassic Sequences, Mass Extinction and Extreme Climate-Change in Eastern Australian Gondwana. *Gondwana Res.* 28, 61–81. doi:10.1016/j.gr.2014.09.002

Maruoka, T., and Isozaki, Y. (2020). Sulfur and Carbon Isotopic Systematics of Guadalupian-Lopingian (Permian) Mid-panthalassa: δ^{34}S and δ^{13}C Profiles in Accreted Paleo-Atoll Carbonates in Japan. *Isl. Arc* 29, e12362. doi:10.1111/iar.12362

McArthur, J. M., Howarth, R. J., and Bailey, T. R. (2001). Strontium Isotope Stratigraphy: LOWESS Version 3: Best Fit to the Marine Sr-Isotope Curve for 0-509 Ma and Accompanying Look-up Table for Deriving Numerical Age. *J. Geology.* 109 (2), 155–170. doi:10.1086/319243

McArthur, J. M., Howarth, R. J., and Shields, G. A. (2012). Strontium Isotope Stratigraphy. *The Geologic Time Scale* 1, 127–144. doi:10.1016/b978-0-444-59425-9.00007-x

McGee, D., and Mukhopadhyay, S. (2013). "Extraterrestrial He in Sediments: From Recorder of Asteroid Collisions to Timekeeper of Global Environmental Changes," in *The noble Gases as Geochemical Tracers*. Editor P. Burnard (Berlin: Springer), 155–176. doi:10.1007/978-3-642-28836-4_7

Metzger, G. J., Greaver, C. A., Jahren, A. H., Smith, A. H., Sheldon, R. M. H., and au, N. D. (2006). Middle-Late Permian Mass Extinction on Land. *Geol. Soc. America Bull.* 118, 1398–1411. doi:10.1130/B26011.1

Montañez, I. P. (2016). A Late Paleozoic Climate Window of Opportunity. *Proc. Natl. Acad. Sci. USA* 113, 2334–2336. doi:10.1073/pnas.1600236113

Montañez, I. P., and Poulsen, C. J. (2013). The Late Paleozoic Ice Age: An Evolving Paradigm. *Annu. Rev. Earth Planet. Sci.* 41, 629–656. doi:10.1146/annurev.earth.031208.100118

Morante, R. (1996). Permian and Early Triassic Isotopic Records of Carbon and Strontium in Australia and a Scenario of Events about the Permian-Triassic Boundary. *Hist. Biol.* 11 (1–4), 289–310. doi:10.1080/10292389609380546

Moynier, F., Agranier, A., Hezel, D. C., and Bouvier, A. (2010). Sr Stable Isotope Composition of Earth, the Moon, Mars, Vesta and Meteorites. *Earth Planet. Sci. Lett.* 300, 359–366. doi:10.1016/j.epsl.2010.10.017

Neymark, L. A., Premo, W. R., Mel'nikov, N. N., and Emsbo, P. (2014). Precise Determination of δ88Sr in Rocks, Minerals, and Waters by Double-Spike TIMS: a Powerful Tool in the Study of Geological, Hydrological and Biological Processes. *J. Anal. Spectrom.* 29, 65–75. doi:10.1039/C3JA50310K

Ota, A., and Isozaki, Y. (2006). Fusuline Biotic Turnover across the Guadalupian-Lopingian (Middle-Upper Permian) Boundary in Mid-oceanic Carbonate Buildups: Biostratigraphy of Accreted limestone in Japan. *J. Asian Earth Sci.* 26, 353–368. doi:10.1016/j.jseaes.2005.04.001

Payne, J. L., Turchyn, A. V., Paytan, A., DePaolo, D. J., Lehrmann, D. J., Yu, M., et al. (2010). Calcium Isotope Constraints on the End-Permian Mass Extinction. *Proc. Natl. Acad. Sci.* 107, 8543–8548. doi:10.1073/pnas.0914065107

Pearce, C. R., Parkinson, I. J., Gaillardet, J., Charlier, B. L. A., Mokadem, F., and Burton, K. W. (2015). Reassessing the Stable (δ$^{88/86}$Sr) and Radiogenic (^{87}Sr/^{86}Sr) Strontium Isotopic Composition of marine Inputs. *Geochim. Cosmochim. Acta* 157, 125e146. doi:10.1016/j.gca.2015.02.029

Peucker-Ehrenbrink, B., and Fiske, G. J. (2019). A continental Perspective of the Seawater 87Sr/86Sr Record: A Review. *Chem. Geology.* 510, 140–165. doi:10.1016/j.chemgeo.2019.01.017

Rampino, M. R., and Shen, S. Z. (2019). "The End-Guadalupian (259.8 Ma) Biodiversity Crisis: the Sixth Major Mass Extinction?," in *Historical Biology*, 1–7. doi:10.1080/08912963.2019.1658096

Richter, F. M., and DePaolo, D. J. (1988). Diagenesis and Sr Isotopic Evolution of Seawater Using Data from DSDP 590B and 575. *Earth Planet. Sci. Lett.* 90, 382–394. doi:10.1016/0012-821X(88)90137-9

Richter, F. M., Rowley, D. B., and DePaolo, D. J. (1992). Sr Isotope Evolution of Seawater: the Role of Tectonics. *Earth Planet. Sci. Lett.* 109, 11–23. doi:10.1016/0012-821X(92)90070-C

Riebesell, U., Wolf-Gladrow, D. A., and Smetacek, V. (1993). Carbon Dioxide Limitation of marine Phytoplankton Growth Rates. *Nature* 361, 249–251. doi:10.1038/361249a0

Saitoh, M., Isozaki, Y., Ueno, Y., Yoshida, N., Yao, J., and Ji, Z. (2013). Middle-Upper Permian Carbon Isotope Stratigraphy at Chaotian, South China: Pre-extinction Multiple Upwelling of Oxygen-Depleted Water onto continental Shelf. *J. Asian Earth Sci.* 67-68, 51–62. doi:10.1016/j.jseaes.2013.02.009

Saitoh, M., Ueno, Y., Isozaki, Y., Nishizawa, M., Shozugawa, K., Kawamura, T., et al. (2014). Isotopic Evidence for Water-Column Denitrification and Sulfate Reduction at the End-Guadalupian (Middle Permian). *Glob. Planet. Change* 123 , 110–120. doi:10.1016/j.jseaes.2014.06.026

Sano, H., and Nakashima, K. (1997). Lowermost Triassic (Griesbachian) Microbial Bindstone-Cementstone Facies, Southwest Japan. *Facies* 36, 1–24. doi:10.1007/bf02536874

Schopf, T. J. M. (1970). Taxonomic Diversity Gradients of Ectoprocts and Bivalves and Their Geologic Implications. *Geol. Soc. America Bull.* 81, 3765–3768. doi:10.1130/0016-7606(1970)81[3765:tdgoea]2.0.co;2

Scotese, C. R. (2008). PALEOMAP Project. Available at: http://www.scotese.com.

Sedlacek, A. R. C., Saltzman, M. R., Algeo, T. J., Horacek, M., Brandner, R., Foland, K., et al. (2014). 87Sr/86Sr Stratigraphy from the Early Triassic of Zal, Iran: Linking Temperature to Weathering Rates and the Tempo of Ecosystem Recovery. *Geology* 42 (9), 779–782. doi:10.1130/G35545.1

Shen, J.-w., and Kawamura, T. (2001). Guadalupian Algae-Sponge Reefs in Siliciclastic Environments-The Reefs at Lengwu (South China) Compared with the Reef at Iwaizaki (Japan). *Facies* 45, 137–156. doi:10.1007/bf02668108

Shen, S.-Z., and Mei, S.-L. (2010). Lopingian (Late Permian) High-Resolution Conodont Biostratigraphy in Iran with Comparison to South China Zonation. *Geol. J.* 45, 135–161. doi:10.1002/gj.1231

Shen, S.-z., Yuan, D.-x., Henderson, C. M., Wu, Q., Zhang, Y.-c., Zhang, H., et al. (2020). Progress, Problems and Prospects: an Overview of the Guadalupian Series of South China and North America. *Earth-Science Rev.* 211, 103412. doi:10.1016/j.earscirev.2020.103412

Shen, S. Z., and Shi, G. R. (2002). Paleobiogeographical Extinction Patterns of Permian Brachiopods in the Asian-Western Pacific Region. *Paleobiology* 28, 449–463. doi:10.1666/0094-8373(2002)028<0449:pepopb>2.0.co;2

Song, H., Wignall, P. B., Tong, J., Song, H., Chen, J., Chu, D., et al. (2015). Integrated Sr Isotope Variations and Global Environmental Changes through the Late Permian to Early Late Triassic. *Earth Planet. Sci. Lett.* 424, 140–147. doi:10.1016/j.epsl.2015.05.035

Stanley, S. M. (2016). Estimates of the Magnitudes of Major marine Mass Extinctions in Earth History. *Proc. Natl. Acad. Sci. USA* 113, E6325–E6334. doi:10.1073/pnas.1613094113

Stanley, S. M., and Yang, X. (1994). A Double Mass Extinction at the End of the Paleozoic Era. *Science* 266, 1340–1344. doi:10.1126/science.266.5189.1340

Stoll, H. M., and Schrag, D. P. (1998). Effects of Quaternary Sea Level Cycles on Strontium in Seawater. *Geochimica et Cosmochimica Acta* 62, 1107–1118. doi:10.1016/S0016-7037(98)00042-8

Taylor, A. S., and Lasaga, A. C. (1999). The Role of basalt Weathering in the Sr Isotope Budget of the Oceans. *Chem. Geology.* 161, 199–214. doi:10.1016/S0009-2541(99)00087-X

Tierney, K. E. (2010). "Carbon and Strontium Isotope Stratigraphy of the Permian from Nevada and China: Implications from an Icehouse to Greenhouse Transition,". PhD thesis (Columbus: Ohio State University).

Tobita, T., Isozaki, Y., and Hayashi, R. (2018). End of Capitanian (Middle Permian) Patch Reef on a Shallow Marine Shelf in NE South China: Lithostratigraphy of Uppermost Iwaizaki Limestone in the South Kitakami Belt, NE Japan. *J. Geography(Chigaku Zasshi)* 127, 775–794. doi:10.5026/jgeography.127.775

Veizer, J., Ala, D., Azmy, K., Bruckschen, P., Buhl, D., Bruhn, F., et al. (1999). ^{87}Sr/^{86}Sr, δ^{13}C and δ^{18}O Evolution of Phanerozoic Seawater. *Chem. Geol.* 161 (1–3), 59–88. doi:10.1016/s0009-2541(99)00081-9

Veizer, J., and Compston, W. (1974). 87Sr/86Sr Composition of Seawater during the Phanerozoic. *Geochimica et Cosmochimica Acta* 38, 1461–1484. doi:10.1016/0016-7037(74)90099-4

Veizer, J. (1989). Strontium Isotopes in Seawater through Time. *Annu. Rev. Earth Planet. Sci.* 17, 141–167. doi:10.1146/annurev.ea.17.050189.001041

Vollstaedt, H., Eisenhauer, A., Wallmann, K., Böhm, F., Fietzke, J., Liebetrau, V., et al. (2014). The Phanerozoic δ88/86Sr Record of Seawater: New Constraints on Past Changes in Oceanic Carbonate Fluxes. *Geochimica et Cosmochimica Acta* 128, 249–265. doi:10.1016/j.gca.2013.10.006

Wang, W.-q., Garbelli, C., Zheng, Q.-f., Chen, J., Liu, X.-c., Wang, W., et al. (2018). Permian 87 Sr/ 86 Sr Chemostratigraphy from Carbonate Sequences in South China. *Palaeogeogr. Palaeoclimatol. Palaeoecol.* 500, 84–94. doi:10.1016/j.palaeo.2018.03.035

Wang, W., Cao, C. Q., and Wang, Y. (2004). The Carbon Isotope Excursion on GSSP Candidate Section of Lopingian-Guadalupian Boundary. *Earth Planet. Sci. Lett.* 220 (1–2), 57–67. doi:10.1016/s0012-821x(04)00033-0

Wei, H., Chen, D., Yu, H., and Wang, J. (2012). End-Guadalupian Mass Extinction and Neg-Ative Carbon Isotope Excursion at Xiaojiaba, Guangyuan, Sichuan. *Sci.China,Ser.B,Chem.LifeSci.EarthSci* 55, 1480–1488.

Wierzbowski, H., Anczkiewicz, R., Pawlak, J., Rogov, M. A., and Kuznetsov, A. B. (2017). Revised Middle-Upper Jurassic Strontium Isotope Stratigraphy. *Chem. Geology.* 466, 239–255. doi:10.1016/j.chemgeo.2017.06.015

Weidlich, O. (2002). Permian Reefs Re-examined: Extrinsic Control Mechanisms of Gradual and Abrupt Changes during 40 My of Reef Evolution. *Geobios* 35, 287–294. doi:10.1016/S0016-6995(02)00066-9

Wignall, P. B., Bond, D. P. G., Haas, J., Wang, W., Jiang, H., Lai, X., et al. (2012). Capitanian (Middle Permian) Mass Extinction and Recovery in Western Tethys: a Fossil, Facies, and 13C Study from Hungary and Hydra Island (Greece). *Palaios* 27, 78–89. doi:10.2110/palo.2011.p11-058r

Wignall, P. B., ´edrine, S. S., Védrine, D. P. G., Wang, W., Lai, X.-L., Ali, J. R., et al. (2009). Facies Analysis and Sea-Level Change at the Guadalupian-Lopingian Global Stratotype (Laibin, South China), and its Bearing on the End-Guadalupian Mass Extinction. *J. Geol. Soc.* 166, 655–666. doi:10.1144/0016-76492008-118

Woods, A. D., Bottjer, D. J., Mutti, M., and Morrison, J. (1999). Lower Triassic Large Sea-Floor Carbonate Cements: Their Origin and a Mechanism for the Prolonged Biotic Recovery from the End-Permian Mass Extinction. *Geol* 27, 645–648. doi:10.1130/0091-7613(1999)027<0645:ltlsfc>2.3.co;2

Yan, D., Zhang, L., and Qiu, Z. (2013). Carbon and Sulfur Isotopic Fluctuations Associated with the End-Guadalupian Mass Extinction in South China. *Gondwana Res.* 24, 1276–1282. doi:10.1016/j.gr.2013.02.008

Zakharov, Y. D., Panchenko, I. V., and Khanchuku, A. I. (1992). A Field Guide to the Late Paleozoic and Early Mesozoic Circum-Pacific Bio- and Geological Events. *Far-eastern Geol. Inst. Russ. Acad. Sci., Far East. Branch, Vladivostok*, 88.

Zhang, G., Zhang, X., Li, D., Farquhar, J., Shen, S., Chen, X., et al. (2015). Widespread Shoaling of Sulfidic Waters Linked to the End-Guadalupian (Permian) Mass Extinction. *Geology* 43, 1091–1094. doi:10.1130/G37284.1

Conflict of Interest: The authors declare that the research was conducted in the absence of any commercial or financial relationships that could be construed as a potential conflict of interest.

Publisher's Note: All claims expressed in this article are solely those of the authors and do not necessarily represent those of their affiliated organizations, or those of the publisher, the editors and the reviewers. Any product that may be evaluated in this article, or claim that may be made by its manufacturer, is not guaranteed or endorsed by the publisher.